

# Accepted Manuscript

Measurement of Relative Position of Halley VI modules (MORPH): GPS monitoring of building deformation in dynamic regions

David H. Jones, Mike Rose

PII: S0165-232X(15)00207-4  
DOI: doi: [10.1016/j.coldregions.2015.09.010](https://doi.org/10.1016/j.coldregions.2015.09.010)  
Reference: COLTEC 2170

To appear in: *Cold Regions Science and Technology*

Received date: 30 March 2015  
Revised date: 4 September 2015  
Accepted date: 12 September 2015



Please cite this article as: Jones, David H., Rose, Mike, Measurement of Relative Position of Halley VI modules (MORPH): GPS monitoring of building deformation in dynamic regions, *Cold Regions Science and Technology* (2015), doi: [10.1016/j.coldregions.2015.09.010](https://doi.org/10.1016/j.coldregions.2015.09.010)

This is a PDF file of an unedited manuscript that has been accepted for publication. As a service to our customers we are providing this early version of the manuscript. The manuscript will undergo copyediting, typesetting, and review of the resulting proof before it is published in its final form. Please note that during the production process errors may be discovered which could affect the content, and all legal disclaimers that apply to the journal pertain.

# Measurement of Relative Position of Halley VI modules (MORPH): GPS monitoring of building deformation in dynamic regions

David H. Jones<sup>1</sup>, Mike Rose<sup>2</sup>

*British Antarctic Survey, High Cross, Madingley Road, Cambridge*

*E-mail: davnes@bas.ac.uk<sup>1</sup> mcr@bas.ac.uk<sup>2</sup>*

**ABSTRACT.** The Halley VI Antarctic Research station was designed as a series of linked, ski-mounted modules. This makes it possible to relocate the station in the event that changing Antarctic conditions require it. These modules are gradually moving relative to each other, distorting the station configuration and potentially threatening the inter-module connections. In this paper we describe a scalable network of GPS receivers used to monitor this distortion. This network has been installed and operational for two months, and is measuring the relative motion of the modules to an accuracy of 1mm, despite the station and its underlying iceshelf moving meters each day under the influence of ocean tides and glacial flow.

## INTRODUCTION

The Halley Research Station, operated by the British Antarctic Survey, has been located on the Brunt Ice Shelf (BIS) (see Figures 2 and 3) in Antarctica since 1956 [Hemmen, 2010]. The first station was built at the conclusion of the International Geophysical Year Trans-Antarctic Expedition, and its location was determined by the end point of this expedition.

Since 1956, the station has grown from a simple wooden hut (Halley I) to a series of linked, ski-mounted, relocatable modules (Halley VI, see Figure 1) with a staff of ten to twenty occupying the station year-round, and fifty to one hundred in the austral summer. The research at the station has a primary focus on atmospheric and climate sciences, and is the site for many long-term monitoring datasets including the records that first indicated the existence of the Antarctic ozone hole [Farman et al., 1985].

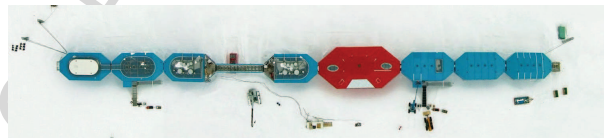


**Fig. 1.** Halley VI research station

As with all large ice shelves in Antarctica, the BIS is continuously supplied with ice flowing from the continent. The surface mass balance of BIS is positive [King et al., 1996], and the mass loss of BIS therefore is predominately caused by calving [Depoorter et al., 2013]. Figure 4 shows the periodic, tidal oscillations of the BIS [Doake et al., 2002], as well as its progression towards the coast.

At its new location, Halley VI is less likely to be lost in a calving event. Nevertheless, the possibility of such an event, even at its new location, can not be completely discounted. For this reason, Halley VI was designed to be mobile. In the event that monitoring activities suggest there is risk of a calving event, it can be dis-assembled into individual modules, towed further inland, then re-assembled.

The eight modules of Halley VI are loosely coupled using flexible links, cables and pipes similar to those that join train carriages. These allow services and staff to pass from one module to another. These flexible links allow for some movement between modules, however in the last few years, movement of some of the modules has been significant. For instance, in 2014 the modules either side of the bridge moved 35cm closer together, putting stress on the bridge fastening points.

The relative movement of the modules is expected, but the precise causes are not fully understood. It is likely due to a combination of factors: for example, differential compaction of the ice beneath the module supports and differential vertical flexing of the station in response to the accumulation of wind-blown snow.

The environmental conditions of Halley mean that adjustments to the positioning of the modules is only possible in the relatively warm summer months so the necessity to realign needs to be predicted well in advance. Continuous monitoring of the relative movement of each module and correlation of those movements with snow topology, operating conditions of the module and environmental conditions may allow for a more detailed understanding of drivers of the movement and hence a minimisation of the realignments.

There exist various automated surveying techniques that could be used for this continuous monitoring, including the use of an automated theodolite, or laser ranging. However these techniques are adversely affected by weather conditions, light

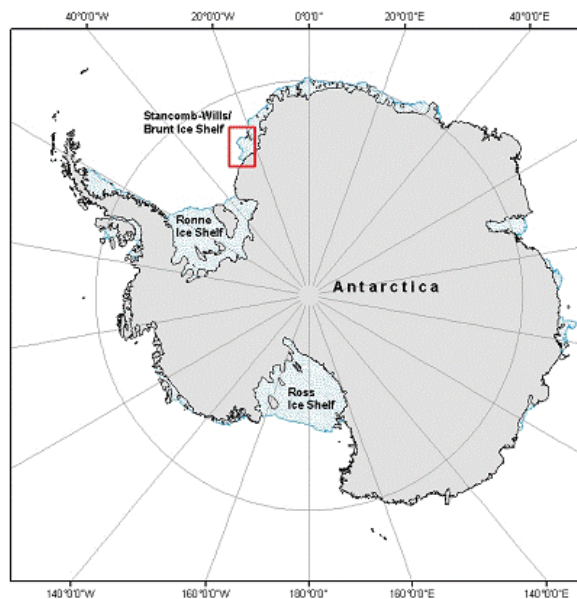


Fig. 2. The location of Brunt Ice Shelf on which the Halley Research Station is located.

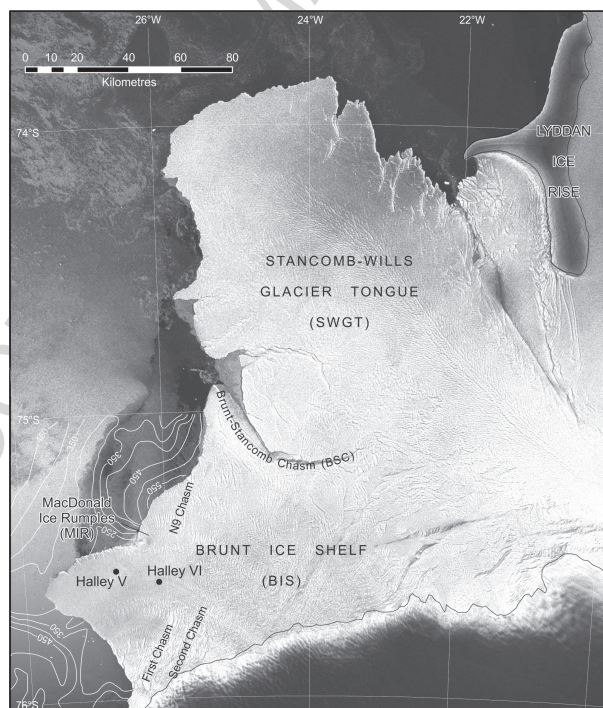


Fig. 3. Location of Halley V and Halley VI on Brunt Ice Shelf.

46 conditions and the accumulation of snow. Also the typical operating temperature range of laser range finders is  $-25^{\circ}\text{C} - 60^{\circ}\text{C}$   
 47 [Pascoal et al., 2008], the operating temperature range of the Leica total station theodolite is  $-20^{\circ}\text{C} - 50^{\circ}\text{C}$ , and external  
 48 temperatures at Halley vary between  $-55^{\circ}\text{C} - 0^{\circ}\text{C}$ .

#### 49 PREVIOUS WORK

50 The first discussions of using GPS for geodetic survey predate the existence of an operational GPS network. Bossler [Bossler  
 51 and Bender, 1980] reports in 1980 that “a highly portable receiver (less than 45 kg and less than 0.07 cubic meter) ... can be  
 52 developed” that may achieve 1-2cm resolution. This was quickly followed with suggestions for how it might effectively be used  
 53 to study tectonic deformation on regional scales [Stolz and Lambeck, 1983]. In 1988 the US Army first proposed measuring the

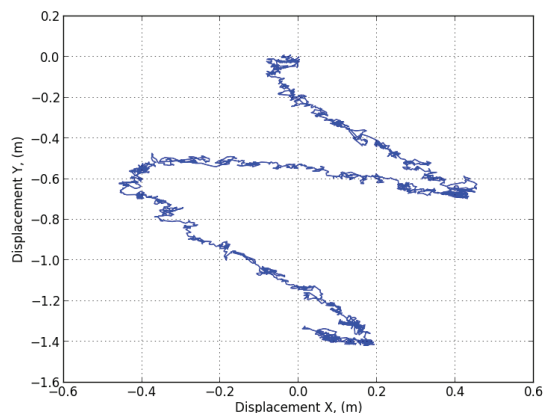


Fig. 4. Example tidal movement and glacial flow of the Brunt Ice shelf, recorded over a period of 24 hours.

54 deformation of infrastructure (the Dworshak Dam in Idaho) with a network of six GPS receivers [DeLoach, 1989]. McLellan  
55 [McLellan et al., 1989] successfully used GPS to study pipeline deformation to sub-centimetre accuracies.

56 The use of GPS to measure the deformation of smaller structures was first proposed in 1995 [Teague et al., 1995]. Since  
57 then it has been used to study the deformation of bridges [Ashkenazi and Roberts, 1997], open pit mines [Stewart et al., 1996]  
58 and tall building [Greulich, 1997]. All of these studies benefited from the proximity of a local reference station. More recent  
59 studies have investigated the use of GPS to measure structure deformation at high frequencies (e.g. [Yi et al., 2012a, 2013]),  
60 and in urban scenarios where near-field multi-path reflections dominate the measurement error [Yi et al., 2011, 2012b].

61 GPS has also been used to study the deformation of dynamic, tidal ice shelves, where the daily deformation is many orders of  
62 magnitude smaller than the tidal movement of the shelf (e.g. [Anderson et al., 2013]). The large separation (tens of kilometres)  
63 of the receivers in these studies restrict the accuracy of their relative measurements to a few centimetres.

## 64 GPS RECEIVER DESIGN

### 65 Requirements and constraints

66 For the purposes of measuring and monitoring module movement, MORPH need only measure their relative positions to an  
67 accuracy of a few centimetres. However, if we are to understand the underlying cause of their relative movement we need to  
68 measure both the separation and alignment of each module to an accuracy in magnitudes of millimetres.

69 Eventually it may be beneficial to instrument all eight modules and the ten auxiliary buildings of Halley. As such, the cost  
70 of each MORPH receiver, and that of any necessary infrastructure modifications, had to be minimal so that this system could  
71 be scaled up to cover the entire station.

72 The installation of the MORPH units required only minor modifications to the infrastructure of Halley. Each MORPH  
73 receiver requires an antenna with a view of the sky, a power supply and a network interface in order to transfer its recordings  
74 to a central computer for processing.

75 The remote location of the station, and its limited internet connectivity, mean that there is also significant benefit to reducing  
76 or eliminating external data transfer requirements.

77 The GPS data processing algorithm will need to be able to filter out the large tidal oscillations of the BIS, and extract the  
78 much smaller movements of the Halley modules.

79 MORPH has two significant advantages that simplify the design over equivalent systems that have been designed for urban  
80 environments:

81 Changes to the loading of each module happen over periods of weeks and months, so it is not necessary to measure the  
82 dynamics of Halley at high frequencies.

83 The surface of the BIS can be assumed to be flat, and the GPS antennas can be mounted high above all the infrastructure  
84 of Halley VI. Moreover, the remote location of the base ensures that there is no other infrastructure nearby. As a result,  
85 any errors introduced by near-field multi-path reflections will be minimal.

### 86 Connectivity

87 The Halley VI station is equipped with a wired local area network with readily accessible ports. These are used to transmit  
88 recorded data from each GPS receiver to a central processing server. Furthermore we can use the Power over Ethernet protocol  
89 to power each receiver from the same cable used for the network interface. This reduces the necessary cabling and thus the  
90 necessary infrastructure modifications.

Module	Power	Accuracy	
		DGPS	RTK
NovAtel OEM628	1.3 W	0.4m	10mm
Trimble BD920	1.3W	0.25m	8mm
Hemisphere Eclipse	2.5W		10mm
Ashtec MB100	0.95W	0.3m	10mm
Septentrio AsteRx2el	2.9W	0.5m	6mm

**Table 1.** Comparison of OEM precision GPS receiver daughter board

### 91 GPS receiver and logger

92 Relative position accuracies up to 2m have been achieved with low cost single-band GNSS receivers [Wiśniewski et al., 2013]  
 93 however we require a greater accuracy so must use the more advanced, but more expensive and more power consuming dual  
 94 band (L1/L2) GNSS receiver. Existing, commercially available, dual-band GNSS receivers are expensive and power consuming  
 95 (Leica GS10: 3.2W, Trimble R8: 2.5W, values from datasheet). The expense of these systems prohibits us from installing a  
 96 large network of them. Instead, our solution is to build an affordable, dedicated receiver and logger with a network protocol  
 97 appropriate to our system requirements.

98 It is not necessary to re-design the sensor from elemental components — there exist various Original Equipment Manufacturer  
 99 (OEM) precision GPS receivers in the form of a daughter board that can be integrated into a larger system. Table 1 compares  
 100 the accuracy (in Differential GPS (DGPS) and onboard Real-Time Kinematic (RTK) position modes) and power consumption  
 101 of five OEM receivers (values from their respective datasheets).

102 The MORPH sensor is built around the Ashtec MB100 L1/L2 GPS receiver board. The MB100 has been chosen over others  
 103 for its acceptable accuracy, low power consumption and low cost.

104 A microcontroller (Micro-robotics VM2) is responsible for configuring the GPS receiver, managing its power supplies,  
 105 monitoring its performance and logging the raw, unprocessed, GPS data on to an SD card. It is also responsible for maintaining  
 106 a network interface to the MORPH server. This interface provides the server with basic monitoring, file management and file  
 107 download facilities.

108 An external Power-Over-Ethernet splitter (TL-POE10R) is used to extract power from the Halley local area network (LAN).  
 109 A Moxa NPort 5150 modem is used to convert the VM2 serial interface into an addressable network port.

110 Figure 5 shows the assembly of each MORPH receiver and Figure 6 shows two MORPH receivers installed at Halley.

111 The cost of this MORPH receiver is approximately £2k, and its power consumption is 1.7W.

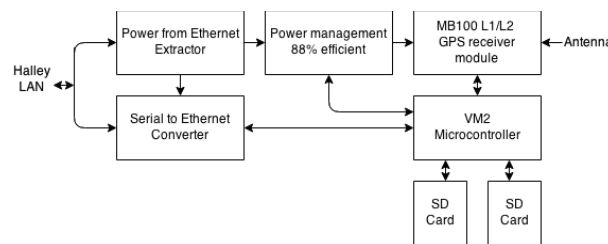


**Fig. 5.** Diagram of MORPH receiver principle components

### 112 MORPH NETWORK ARCHITECTURE

113 Each GPS receiver stores the unprocessed GPS data in the compressed Ashtec ATOM format [Artushkin et al., 2008]. 24 hour  
 114 segments of data are recorded into individual files on to an SD card. The MORPH server can interrogate each receiver for  
 115 detail of its performance, its status and perform basic file management tasks and downloads.

116 Every day the server polls each receiver for a list of the files it has generated, then downloads any new files. This compressed  
 117 data is then converted into the RINEX format with an Ashtec utility. Finally the RINEX files are analysed to generate a time  
 118 series of daily relative positions. This is a fully automated procedure which requires no external internet connectivity.



Fig. 6. Two MORPH receivers installed at Halley

## 119 GPS DATA PROCESSING TECHNIQUES

120 The pseudorange and carrier-phase measurements for each GPS satellite and for each MORPH receiver are captured in the  
 121 RINEX files saved to the MORPH server each day. There exist various methods for converting this data into useful position  
 122 and distance measurements. A common method is to compare this data to that received from a nearby GPS receiver station  
 123 with a known location, such as those of the International GNSS Service (IGS). This forms a baseline from which a position can  
 124 be calculated relative to that of the known station location. This is not suitable for many Antarctic measurements, including  
 125 those of this network, because of the dynamic nature of the Antarctic ice sheet — there are few places suitable to setup a  
 126 stationary receiver. The closest IGS station to the MORPH network is 2600 km away at the SANAE IV Antarctic research  
 127 station.

128 Precise Point Positioning (PPP) is an alternative analysis method which relies upon the precise satellite orbit and clock  
 129 measurements from IGS. These are used to fit a static or kinematic receiver model to the un-differenced satellite observations  
 130 of the receiver. Static PPP is typically two orders of magnitude more precise than kinematic PPP, however the BIS is moving  
 131 at speeds many orders of magnitude greater than the distances we need to measure, so a static PPP solution will be dominated  
 132 by the movement of the BIS. Kinematic precise point positioning is used to measure the movement and distortion of BIS as  
 133 part of the Lifetime of Halley [Anderson et al., 2013] network to a centimetre accuracy.

134 Another processing method suitable for MORPH is double-differencing. Double-differencing is a carrier-signal relative posi-  
 135 tioning algorithm; this is a powerful technique for processing data from receivers nearby to each other. This technique removes  
 136 most of the common errors between different signal paths, including clock-biases and atmospheric effects, making it possible  
 137 to accurately measure the phase of each GPS satellite carrier-wave [Laurichesse, 2011]. It is then necessary to discriminate  
 138 between the different carrier-wave cycles, or integer ambiguities, of each satellite. The Real-Time Kinetic LIBrary (RTKLIB) is  
 139 a compact and portable program library that performs double difference GPS calculations [Takasu and Yasuda, 2009] and then  
 140 resolves the integer ambiguities with the LAMBDA (Least-squares AMBIGuity Decorrelation Adjustment) method [Teunissen,  
 141 1995].

142 RTKLIB has been used to calculate sub-decimeter accuracies in kinematic scenarios [Bäumker et al., 2013]. Unlike Baumker's  
 143 application of RTKLIB to unmanned aerial vehicle movement in urban areas, MORPH has some advantages that may mean  
 144 we can improve upon this accuracy:

- 145 1. The GPS antenna used by each MORPH sensor is a Leica AS10. This is a survey-quality geodetic antenna with good  
 146 multi-path rejection performance [Stephenson et al., 2001]. Furthermore the antenna has an unobstructed view of the sky,  
 147 maximising satellite coverage whilst minimising multi-path reflections.
- 148 2. The MORPH sensors record GPS satellite data every 10s. The distortion of the Halley modules is happening over weeks  
 149 and months, as such we only need one measurement each day. This means we can extensively filter outlier datapoints and  
 150 still calculate an average relative position from a large dataset.
- 151 3. In order to measure the alignment of each Halley module, two MORPH sensors are fitted to each module. This has  
 152 the additional advantage that their separation is fixed and known a-priori. This measurement can be used to compute  
 153 the accuracy of the two receivers on a daily basis, as well as to ensure there are no systematic errors in the processing  
 154 algorithm.

155 The RTKLIB - RTK2RTKP program is executed with the following non-default configuration parameters:

Position mode	Moving Baseline
Elevation mask	0 degrees
SNR mask	0 dBHz
Ionosphere correction	L1-L2 combination
Troposphere correction	Estimate Zenith total delay and horizontal gradient
Integer ambiguity resolution	Continuous

157 The 10s interval output from RTK2RTKP is then filtered against the following criteria:

- 158 1. The estimated standard deviations of the solution assuming a priori error model and error parameters by the positioning  
 159 options. If this is below 0.01m in the X-Y plane, and 0.05m in the Z plane, the output is accepted.
- 160 2. If the solution is a relative carrier-based position with a properly resolved integer ambiguity, the output is accepted.
- 161 3. The validity of the integer ambiguity resolution, as measured by the “ratio test” [Euler and Schaffrin, 1991]. This is the  
 162 ratio of the squared norm of the “second-best” ambiguity residual vector and the squared norm of the “best” ambiguity  
 163 residual vector. The greater the ratio, the greater confidence there is in the solution. If this value is greater than 10, the  
 164 output is accepted.

165 Figure 7 compares the performance of the RTKLIB analysis, with and without filtering its output against these performance  
 166 criteria. Note that the algorithm error is defined here as variation in the distance between two antennas of fixed (approximately  
 167 12m) separation, and that this metric is not part of the filtering criteria.

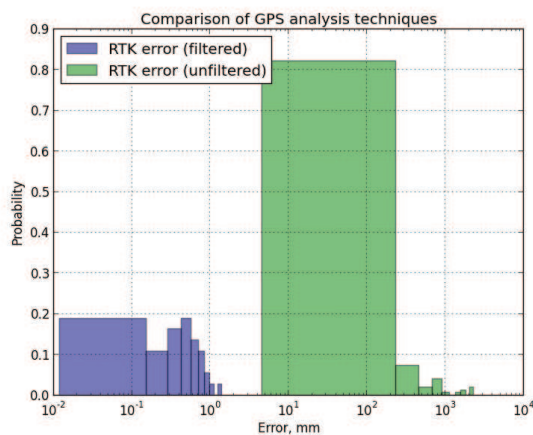


Fig. 7. A comparison of the accuracy of RTK processing using RTKLIB, before and after filtering the output

168 Figure 8 compares the performance of the GIPSY/OASIS Static PPP and Kinematic PPP, and the RTKLIB Double  
 169 differencing analysis. As expected, the static PPP method error is dominated by the daily movement of the ice-shelf. Figure  
 170 4 shows this sinusoidal tidal movement and the glacial flow, as measured with Kinematic PPP processing of data from a  
 171 MORPH module. The position error visible in this graph is much smaller than the error the tidal movement induces in a

172 static analysis, and so the error in the distances measured by the MORPH network is correspondingly improved. However the  
 173 RTKLIB accuracy is another couple of orders of magnitude better than that of Kinematic PPP.

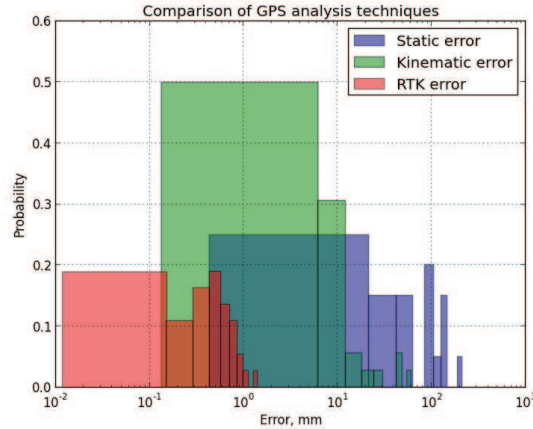


Fig. 8. A comparison of the accuracy of Static (PPP), Kinematic and RTK processing techniques using GIPSY/OASIS and RTKLIB

## 174 INITIAL RESULTS

175 For the purposes of MORPH, the geocentric coordinate system is less relevant, instead we project the data onto a set of axis  
 176 where the x-axis is aligned with a bearing between the antennas at either end of Halley.

177 This projection assumes that the small area of interest can be treated as a 2-D cartesian plane. The X and Y separation (in  
 178 geocentric co-ordinates) of the antennas at either end of Halley are determined using the aforementioned RTKLIB process.  
 179 An angle ( $\theta$ ) is calculated such that, when these antenna locations are rotated about another antenna approximately half way  
 180 between the two at  $(x_0, y_0)$ , the new Y separation between the antennas is 0. Thus this baseline becomes the X-axis. The Y  
 181 axis is orthogonal to this baseline, and the origin is  $(x_0, y_0)$ . The remaining antenna locations can then be projected onto this  
 182 set of axis using the transformation:

$$\begin{bmatrix} x' \\ y' \end{bmatrix} = \begin{bmatrix} \cos(\theta) & -\sin(\theta) \\ \sin(\theta) & \cos(\theta) \end{bmatrix} \begin{bmatrix} x - x_0 \\ y - y_0 \end{bmatrix} \quad (1)$$

183 Figure 9 shows the layout of four MORPH GPS receivers, two on each of two Halley modules. The modules themselves are  
 184 separated by a bridge.

185 Figures 10–12 shows the relative movement as measured by these MORPH receivers. Line S2–S3 shows the relative move-  
 186 ment between the two receivers that straddle the gap between the modules. Lines S1–S2 and S3–S4 shows the rotation of  
 187 the modules, which is also shown in figure 13 in degrees relative to the overall station orientation.

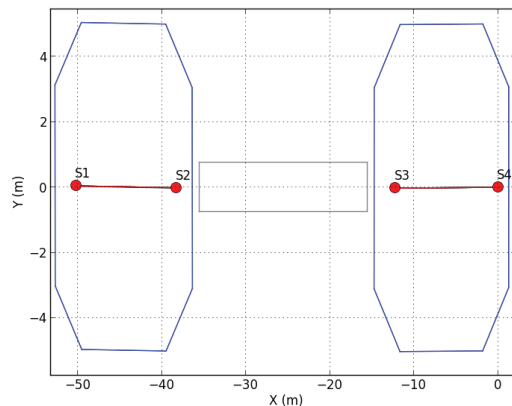


Fig. 9. Location of antennas on two modules

188 From these figures we can see that the gap between the two modules is shrinking at almost 1mm per day. The minor changes  
 189 in alignment between the modules is also evident, as is the slow sinking and tipping of the right hand module.

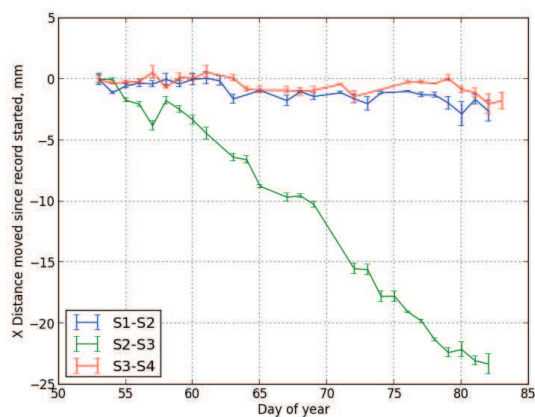


Fig. 10. Initial data showing the relative movement of two modules in X axis

## 190 CONCLUSIONS

191 Twelve MORPH receivers are now installed in six Halley VI modules and an external laboratory. This network of receivers is  
 192 providing a high quality record of the movement of modules and the overall distortion of the Halley VI station. The MORPH  
 193 system is cost-effective, and its installation has had little impact on the station infrastructure and its operations. MORPH is

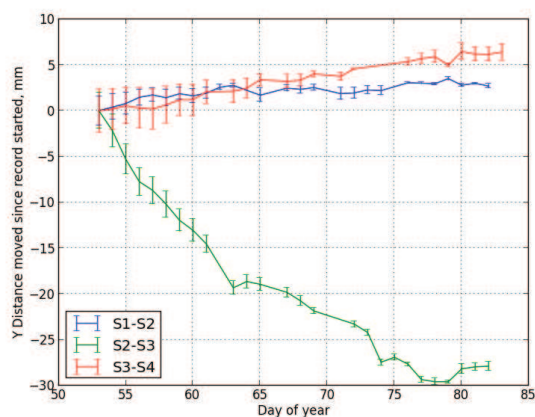


Fig. 11. Initial data showing the relative movement of two modules in Y axis

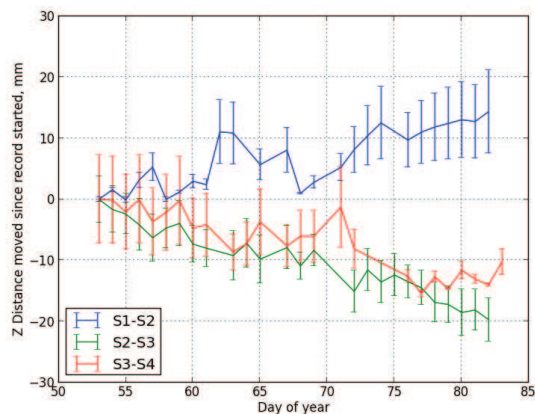


Fig. 12. Initial data showing the relative movement of two modules in Z axis

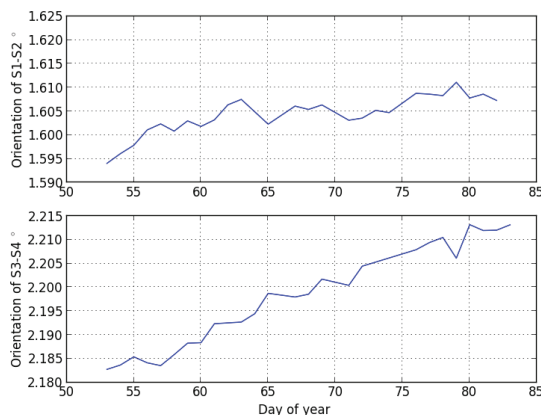


Fig. 13. Initial data showing the rotation of two modules

194 now providing the occupants and operations managers of Halley VI with the data they need to manage the risk, and understand  
 195 the causes, of the relative module movement.

## 196 REFERENCES

- 197 R. Anderson, D. H. Jones, and G. H. Gudmundsson. Halley research station, antarctica: calving risks and monitoring strategies. *Natural*  
 198 *Hazards and Earth System Sciences*, 1:6227–6256, 2013.
- 199 I. Artushkin, A. Boriskin, and D. Kozlov. Atom: Super compact and flexible format to store and transmit gnss data. *Proc ION GNSS*,  
 200 pages 1895–1902, 2008.
- 201 V. Ashkenazi and G. W. Roberts. Experimental monitoring of the humber bridge using gps. *Proceedings of the ICE - Civil Engineering*,  
 202 120(4):177–182, 1997.
- 203 M Bäumker, HJ PRZYBILLA, and A Zurhorst. Enhancements in uav flight control and sensor orientation. In *Conference on Unmanned*  
 204 *Aerial Vehicles in Geomatics, Rostock, Germany*, 2013.
- 205 J. D. Bossler and P. L. Bender. Using the global positioning system (gps) for spatial positioning. *Bulletin Geodesique*, 54:553–563, 1980.
- 206 Stephen R DeLoach. Continuous deformation monitoring with gps. *Journal of Surveying Engineering*, 115(1):93–110, 1989.
- 207 M. A. Depoorter, J. L. Bamber, J. A. Griggs, J. T. M. Lenaerts, S. R. M. Ligtenberg, M. R. van den Broeke, and G. Moholdt. Calving  
 208 fluxes and basal melt rates of antarctic ice shelves. *Nature*, 502:8992, 2013.
- 209 C. S. M. Doake, H. F. J. Corr, K. W. Nicholls, A. Gaffikin, A. Jenkins, W.I. Bertiger, and M. A. King. Tide-induced lateral movement  
 210 of Brunt ice shelf. *Geophysical Research Letters*, 29, 2002.
- 211 H. J. Euler and B. Schaffrin. On a measure for the discernibility between different ambiguity solutions in the static-kinematic gps-mode.  
 212 *IAG Symposia*, 107:285–295, 1991.
- 213 J. C. Farman, B. G. Gardiner, and J. D. Shanklin. Large losses of total ozone in Antarctica reveal seasonal ClOx/NOx interaction.  
 214 *Nature*, 315:207–210, 1985.
- 215 G. Greulich. Discussion: Dynamic deformation monitoring of tall structure using gps technology. *Journal of Surveying Engineering*, 123  
 216 (1):49–50, 1997. doi: 10.1061/(ASCE)0733-9453(1997)123:1(49).
- 217 G. E. Hemmen. Royal Society expeditions in the second half of the twentieth century. *Notes and Records of the Royal Society*, 2010.
- 218 J. C. King, P. S. Anderson, C. Smith M., and S. D. Mobbs. The surface energy and mass balance at halley, antarctica during winter.  
 219 *Journal of Geophysical research*, 101:19119–19128, 1996.
- 220 D. Laurichesse. The CNES Real-Time PPP with undifferenced integer ambiguity resolution demonstrator. *ION GNSS*, 2011.
- 221 J. McLellan, T. Porter, and P. Price. Pipeline deformation monitoring using gps survey techniques. *Journal of Surveying Engineering*,  
 222 115(1):56–66, 1989. doi: 10.1061/(ASCE)0733-9453(1989)115:1(56).
- 223 J. Pascoal, L. Marques, and A. T. Almeida. Assessment of laser range finders in risky environments. *Intelligent Robots and Systems*,  
 224 pages 3533–3538, 2008.
- 225 Scott Stephenson, Xiaolin Meng, Terry Moore, Anthony Baxendale, and Tim Edwards. Implementation of v2x with the integration of  
 226 network rtk: Challenges and solutions. pages 1556–1567, 2001.
- 227 M. P. Stewart, M. Tsakiri, and X. Ding. Gps navigation techniques in open pit deformation monitoring. *Proceedings of ION GPS*, pages  
 228 1225–1231, 1996.
- 229 A. Stolz and K. Lambeck. Geodetic monitoring of tectonic deformation in the australian region. *Journal of the Geological Society of*  
 230 *Australia*, 30:411–422, 1983.
- 231 T. Takasu and A. Yasuda. Development of the low-cost rtk-gps receiver with an open source program package rtklib. *International*  
 232 *Symposium on GPS/GNSS*, 2009.
- 233 E Harrison Teague, Jonathan P How, London G Lawson, and Bradford W Parkinson. Gps as a structural deformation sensor. 1995.
- 234 P. J. Teunissen. The least-squares ambiguity decorrelation adjustment: a method for fast gps integer ambiguity estimation. *Journal of*  
 235 *Geodesy*, 70(1-2):6582, 1995.

- 236 B. Wiśniewski, K. Bruniecki, and M. Moszyński. Evaluation of RTKLIB's Positioning Accuracy Using low-cost GNSS Receiver and  
237 ASG-EUPOS. *International Journal on Marine Navigation and Safety of Sea Transportation*, 7(1), 2013.
- 238 T-H. Yi, H-N. Li, and M. Gu. Characterization and extraction of global position system multipath signals using particle filtering algorithm.  
239 *Measurement Science and Technology*, 22:75101–75111, 2011.
- 240 T-H. Yi, H-N. Li, and M. Gu. Recent research and applications of GPS-based monitoring technology for high-rise structures. *Structural*  
241 *Health and Monitoring*, 20:649–670, 2012a.
- 242 T-H. Yi, H-N. Li, and M. Gu. Effect of different construction materials on propagation of GPS monitoring signals. *Measurement*, 45:  
243 1126–1139, 2012b.
- 244 T-H. Yi, H-N. Li, and M. Gu. Experimental assessment of high-rate GPS receivers for deformation monitoring of bridge. *Measurement*,  
245 46:420–432, 2013.